NASA Technical Paper 1400

The Design of Supercritical Wings by the Use of Three-Dimensional Transonic Theory

Michael J. Mann

FEBRUARY 1979

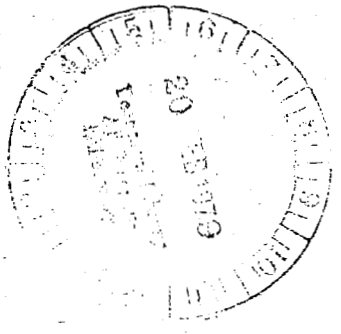

NASA

NASA Technical Paper 1400

The Design of Supercritical Wings by the Use of Three-Dimensional Transonic Theory

Michael J. Mann
Langley Research Center
Hampton, Virginia

National Aeronautics
and Space Administration

**Scientific and Technical
Information Office**

1979

SUMMARY

A procedure has been developed for the design of transonic wings by the iterative use of three-dimensional, inviscid, transonic analysis methods. The procedure is based on simple principles of supersonic flow and provides the designer with a set of guidelines for the systematic alteration of wing profile shapes to achieve some desired pressure distribution. The method is generally applicable to wing design at conditions involving a large region of supercritical flow. To illustrate the method, it is applied to the design of a wing for a supercritical maneuvering fighter that operates at high lift and a transonic Mach number. The wing profiles were altered to produce a large region of supercritical flow which is terminated by a weak shock wave. The spanwise variation of drag of this wing and some principles for selecting the streamwise pressure distribution are also discussed.

INTRODUCTION

The early methods developed for the design of swept wings at transonic speeds relied almost entirely on linear theory (refs. 1 to 6). The successful use of linear theory for the design of high-aspect-ratio transonic configurations is reported in references 5 and 6.

Current transonic-wing design procedures (refs. 7 and 8, for example) utilize the general framework of linearized theory as outlined in references 2 to 6. However, difficulties can occur with this approach, especially for high lift and highly three-dimensional shapes. For example, wind-tunnel tests of references 8 and 9 showed the existence of strong shock waves on the wings of configurations designed by the use of linear theory.

Considerable progress has recently been made in the development of theoretical methods for analyzing transonic flows. Efforts have been under way for some time to incorporate two-dimensional and three-dimensional transonic computational methods into the wing design process (refs. 8 to 12). Some of this work has resulted in improvements to designs which were initially defined on the basis of linear theory.

Another promising development is numerical optimization (refs. 13 to 16). This approach is based on the coupling of a transonic aerodynamic analysis method with an optimization method. In this way, the wing profile shapes which optimize some aerodynamic property within a set of constraints can be determined. The constraints can be used to meet off-design requirements.

The purpose of the present study is to develop a definite procedure for the design of transonic wings which utilizes three-dimensional transonic analysis methods in an iterative fashion. The design procedure is based on the aerodynamic principles of supersonic flow and therefore applies to those conditions involving a large region of supercritical flow. The procedure provides

the designer with a set of guidelines for the systematic alteration of wing profile shapes to achieve some desired pressure distribution.

The procedure is illustrated by the design of the wing for a fighter that operates at transonic maneuver conditions. The planform and twist distribution are fixed and the wing profile shapes are altered to produce a large region of supercritical flow which is terminated by a weak shock wave. The flow is assumed to remain attached. It is recognized that the practical application of the maneuver shape to an aircraft would require the use of variable geometry.

This study also presents some principles for selecting the streamwise pressure distribution on a transonic maneuvering fighter and examines the spanwise variation of inviscid drag on the final wing design.

SYMBOLS AND ABBREVIATIONS

b wing span, m

C_D total drag coefficient, $\frac{\text{Drag}}{q_\infty S}$

C_L total lift coefficient, $\frac{\text{Lift}}{q_\infty S}$

C_p pressure coefficient, $\frac{p - p_\infty}{q_\infty}$

c local chord length, m

c_{av} average chord, $\frac{b}{\text{Aspect ratio}}$, m

c_d section drag coefficient

Δc_d c_d at $M_\infty = 0.90$ less c_d at $M_\infty = 0.01$

c_l section lift coefficient

M local Mach number

M_n local Mach number normal to local sweep line, $M \cos \Lambda$

M_∞ free-stream Mach number

p static pressure, Pa

p_∞ free-stream static pressure, Pa

q_∞ free-stream dynamic pressure, Pa

S wing area, m^2

SMF supercritical maneuvering fighter

t time, sec

t/c maximum thickness ratio

x,y,z Cartesian coordinates in the streamwise, spanwise, and vertical directions, respectively, m

α angle of attack, deg

γ ratio of specific heats, = 1.4

η = y/(b/2)

Λ local sweep angle, deg

Superscript:

* critical Mach number conditions

Subscript:

vac vacuum

BASIC THEORETICAL CONCEPTS

Transonic flow is inherently nonlinear and highly three-dimensional for bodies of finite span. Due to the nonlinearity, the flow cannot be divided into the effects of thickness and camber, as can be done in the case of linear theory. Rather, transonic flow requires the solution of a nonlinear partial differential equation and the careful control of the body surface coordinates or, in particular, of the surface curvature.

Near sonic speeds, the flow disturbances propagate forward at about the same speed as the body which creates the disturbances. However, the lateral flow has an incompressible character; that is, the stream tubes have a strong resistance to change in area but not to changes in curvature or displacement (ref. 17). This strong lateral effect makes the three-dimensional effects of finite span a maximum at $M_\infty = 1$ (and also leads to the transonic area rule).

Aside from the shock-wave—boundary-layer interaction problem, boundary-layer displacement effects tend to be of particular importance for transonic designs. Supercritical airfoils generally develop a large amount of aft loading. These loadings correspond to pressure distributions which thicken the upper surface boundary layer at the trailing edge and therefore reduce the effective camber in the aft region (ref. 18). Furthermore, the boundary layer

can have an influence on the three-dimensional nature of the flow since the boundary layer is a region of low-speed flow which does not exhibit lateral incompressibility (ref. 17).

The inviscid drag of a transonic wing is, of course, composed of the usual induced drag and wave drag components (refs. 19 to 21). The wave drag is calculated by an integral of certain quantities over the shock wave and is zero if the shock strength is zero. The shock wave is an irreversible compression of the flow which results in a pressure distribution that gives wave drag. Thus, if the wing were designed to compress the flow isentropically, the wave drag would be zero.[1]

It is of interest to note that an equivalent situation apparently exists in the case of supersonic flow over a body. For this case, Von Kármán (ref. 22) indicates that a solution of the exact nonlinear flow equations would show that the wave drag was due to a change in momentum which is caused by the shock waves.

Viscous drag resulting from the well-known shock-induced boundary-layer separation is the dominant problem associated with the shock wave. This separation causes a rapid drag rise, buffet, and stability problems (refs. 18 and 23). In the case of fighter aircraft, this shock-induced separation reduces the maneuverability and therefore the combat effectiveness.

Due to the considerable adverse effects of the shock wave on transonic aircraft performance, the present study has focused on the development of a systematic approach to designing transonic wings with weak shock waves. Since three-dimensional transonic design methods are not yet available, a three-dimensional transonic analysis method was used. The FLO 22 computer program of Jameson and Caughey (refs. 24 and 25) was used. Their program solves the full potential flow equations and imposes the exact boundary conditions.

A fighter wing has been designed for the transonic maneuvering condition. Although the conditions for which the FLO 22 computer program have been experimentally validated might not encompass the design conditions for this wing, the theory is believed to be sufficiently accurate to demonstrate the design principles. The fighter wing was designed to develop a large region of supercritical flow which is terminated by a weak shock wave. The desired flow pattern was achieved by extensive iteration on the profile shapes at the various span stations. On each iteration, the pressure distribution was examined and the profile shapes were altered according to the definite iteration procedure. The procedure is based on the principles governing the compression and expansion of the supersonic flow on the upper surface of the wing.

---

[1]This approach is in contrast to the crest approach (the crest is the location where the tangent to the surface is parallel to the free-stream velocity), which seeks to position the shock at or ahead of the crest in order to avoid drag divergence. What is needed is to reduce the shock strength, and then the pressure distribution will automatically adjust to reduce wave drag.

DESIGN OF A TRANSONIC WING

Problem Definition

In this section, the starting configuration for the design of a wing for a supercritical maneuvering fighter (SMF) is discussed. The present study is restricted to the design of an isolated wing.

An iterative wing design method necessarily requires some initial or starting configuration. The starting configuration for the present study is the SMF-1 wing described in reference 26. This wing was also described in a talk entitled "Design and Validation of a High-Lift Transonic Airfoil" given by S. K. Hadley, M. J. Mann, and J. C. Ferris at the NASA Conference on Advanced Technology Airfoil Research at Langley Research Center in March 1978. The planform is typical of many current high-performance combat aircraft and is shown in figure 1. The wing profile shapes were designed primarily by a two-dimensional strip theory. The twist distribution is shown in figure 2. The design point for SMF-1 and for the current design, SMF-2, is $M_\infty = 0.90$ and $C_L = 0.86$.

In order to evaluate the result of the strip theory approach, the pressure distribution of SMF-1 at the design point was estimated with the three-dimensional transonic theory and is shown in figure 3. The results described in the previously mentioned talk indicated that this design resulted in measurable improvements over a wing developed in an earlier study. However, in view of the flow expansion ahead of the shock wave and the strong shock extending all the way across the wing as indicated by figure 3, it was felt that additional improvements could be achieved by applying the three-dimensional transonic theory to the design.

The SMF-2 wing was designed by modifying the wing profiles of SMF-1. The objective was to achieve the design Mach number and lift coefficient with reduced shock strength. The planform of figure 1 was held fixed. The twist distribution was determined by a vortex-lattice theory in a manner similar to that described in reference 27 (fig. 2). The twist distribution was also held fixed.

Target Pressure Distribution

In order to reduce the shock strength and to achieve the required high lift, an upper surface target pressure distribution was chosen in which the flow expands rapidly at the leading edge and isentropically compresses as it proceeds toward the trailing edge. Since the flow must compress toward stagnation conditions at the trailing edge, the only way to simultaneously achieve both the highest lift possible and a low Mach number just upstream of the shock is to have this type of sloped pressure distribution. Once the normal Mach number upstream of the shock is reduced by decelerating or compressing the flow ahead of the shock, the strength of the shock is reduced. In order to avoid leading-edge separation, the leading-edge pressure coefficient will be limited to 0.7 times the vacuum pressure coefficient. The vacuum pressure coefficient ($p = 0$) is given by

$$C_{p,vac} = -\frac{2}{\gamma M_\infty^2} \tag{1}$$

Another argument for this type of sloped pressure distribution is based on the shape of the planform in figure 1. The pressure coefficient on an infinite swept wing is

$$C_p = \frac{p - p_\infty}{q_\infty} = \frac{2}{\gamma M_\infty^2}\left[\left(\frac{1 + \frac{\gamma - 1}{2} M_\infty^2 \cos^2 \Lambda}{1 + \frac{\gamma - 1}{2} M_n^2}\right)^{\frac{\gamma}{\gamma-1}} - 1\right] \tag{2}$$

where Λ is the sweep angle and $M_n = M \cos \Lambda$ is the Mach number normal to the wing at the point where C_p is measured. If this concept is applied locally to the finite tapered wing where Λ becomes the local sweep of a constant percent chord line, the variation in critical pressure coefficient C_p^* across the wing can be computed by setting $M_n = 1$. The result for the present planform is shown by the dashed lines in figure 3.

The variation of C_p^* shown in figure 3 indicates that if a shock wave were to occur near the trailing edge of this planform, it would be a strong shock in the case of either a constant or an increasingly negative streamwise pressure distribution since the shock will probably be almost normal and will compress the flow to subcritical speeds. This is, in fact, the case with SMF-1. In effect, the trailing edge of the wing does not have much sweep benefit. Therefore, with a trailing-edge shock wave, this variation in C_p^* also suggests a beneficial effect from the sloped pressure distribution (i.e., decreasingly negative streamwise; see refs. 28 to 30).

Off-design performance for this sloped pressure distribution would be somewhat reduced and would therefore require variable geometry. Since the purpose of this study is to determine the available degree of benefit that might be obtained at the maneuver condition, any practical limitations that might be encountered with the required variable geometry are not allowed to restrict the wing shape.

Design Procedure

This section describes the techniques used to modify the upper surface curvature of a streamwise profile on the SMF-1 wing to provide the desired sloped pressure distribution and reduced shock strength at the design maneuver condition.

The three-dimensional flow field around a wing is established by the sound or pressure waves generated by the wing. These pressure waves exist, of course, in both the subsonic and the supersonic regions of the flow. However, in the supersonic regions, the zone of influence of a compression wave or an expansion wave is limited and its effect is more easily defined. It is necessary to establish the relationship between the wing geometry and the type of waves generated by the wing surface and then to visualize the effects of these waves on the flow over the wing. It will then be possible to design for a target pressure distribution on the wing by iteration on the streamwise surface curvature.

Figure 4 illustrates the transonic flow over a streamwise profile of a wing. The flow has an embedded region of supersonic flow which is terminated by a shock wave. The chordwise length is divided into three regions which are used in the design process. The use of each region will be explained and illustrative examples will be given.

For the sake of clarity, figure 4 shows only an idealized wave pattern caused by an expansion at the leading edge. This demonstrates the well-known effect of rapid expansion to supersonic velocities and low pressures at the leading edge of an airfoil with an embedded region of supersonic flow (refs. 29 and 30). As the flow accelerates around the nose, it generates expansion waves which reflect from the sonic line as compression waves. These compression waves in turn reflect from the airfoil surface as more compression waves. Although the extent and location of the compression would depend on such quantities as the airfoil geometry and angle of attack, the effect of the airfoil leading-edge region is to first expand the flow and then compress it.

The level of the suction peak near the leading edge can be controlled by adjustment to the camber and the upper surface curvature in the first few percent of the wing chord. The leading-edge suction peak near the root of SMF-1 was eliminated by increasing curvature in this region while holding the thickness constant. This amounted to a reduction in the local angle of attack of the wing leading edge.

In the middle region of the wing profile, between the leading edge and the shock wave as shown in figure 4, the pressure is determined by the combined influence of the reflected leading-edge disturbances and disturbances originating from the surface in this region. The effect of the surface on the pressure in this region can essentially be visualized as a Prandtl-Meyer flow; that is, depending on the direction of the streamwise curvature, the surface either isentropically compresses or expands the flow. A decrease in curvature[2] (convex looking from outside of the profile) will decrease the expansion produced by the surface itself. Thus, in order to achieve the desired isentropic compression ahead of the shock wave, the upper surface curvature of SMF-1 needs to be decreased in the middle region. In fact, it may even be necessary to have a reflex in the surface (a reverse in curvature) so that the surface becomes

---

[2]As used in this report, the term "curvature" is used to refer to curvature which is convex, the normal streamwise curvature of the upper surface of a wing. Thus, a decrease in curvature could even mean an increase in concavity of a reflexed or saddleback profile shape.

concave for some distance and adds further compression to any useful compression produced by the leading edge.

The final region downstream of the shock wave can be used to obtain further reductions in shock strength and to simultaneously gain additional lift. There are numerous situations in fluid mechanics in which an expansion wave interacts with a shock wave and reduces the strength of the shock. The simplest illustration of this is the one-dimensional flow of a piston moving down a cylinder. Assume that a piston has started from rest and is impulsively accelerated to some velocity. A shock wave will be generated which also moves down the cylinder, only at a much higher velocity than the piston.

Figure 5 shows this flow at a later time when the piston has made a gradual deceleration for a short period of time. The fluid motion is illustrated in both the time-distance plane and the physical plane. As the piston decelerates, it produces expansion waves which always catch up to the shock wave, merge with it, and reduce its strength (ref. 31).

Considering this phenomenon in relation to the three-dimensional transonic wing problem suggests an increase in the upper surface curvature downstream of the shock wave. This increase in curvature should expand the flow and further reduce the shock strength. The new flow pattern will be one in which the flow just downstream of the shock is expanded to lower pressures and the shock strength is reduced.

Figures 6 and 7 show two examples of profile modification which illustrate the concepts just outlined. The changes in pressure distribution are correlated with the changes in upper surface slope and curvature at the given spanwise station. Excepting the nose region where geometric slopes are large, the slope of the dz/dx plot is approximately proportional to the surface curvature.

Figure 6 shows the effect of only a decrease in the surface curvature in the middle region and figure 7 shows the effect of only an increase in the surface curvature at and downstream of the shock. Both changes weakened the shock. Notice that an increase in curvature moved the shock aft and a decrease in curvature moved the shock forward.

The procedure described here was applied at a given span station, based primarily on the chordwise pressure distribution at that span station. It was found that the spanwise propagation of disturbances created by changes in geometry was stronger in the outboard direction. (The reverse is true for a swept-forward wing.) Thus, the spanwise variation in profile shape was determined by starting at the root and progressing toward the tip.

The actual implementation of this design procedure required a computer program in which the changes in slope of a given profile were specified and new surface coordinates were calculated. As indicated in the lower portions of figures 6 and 7, a smooth chordwise variation in the increment to the surface slopes is required in order to produce a change in curvature. Once a new upper surface shape was determined, the old profile thickness distribution was subtracted from the new upper surface coordinates to determine the new lower

surface coordinates. Since the twist distribution was held fixed during the design process, the wing angle of attack had to be adjusted as the profile shapes were changed in order to maintain the design C_L.

The first step in the design process is to obtain a converged solution on the initial or starting configuration with the three-dimensional transonic theory. In the case of the FLO 22 computer program, it was found that 200 iterations with a crude grid (96 streamwise, 12 normal, and 16 spanwise computational grid points) and several hundred more iterations with a fine grid (192 streamwise, 24 normal, and 32 spanwise) were needed to obtain a converged solution. Convergence was determined by examining the changes in the pressure distribution and shock location as the program iterated. Once a single converged solution was obtained and stored in the computer memory, the solution for each subsequent perturbed wing shape could generally be obtained by starting with the converged solution for the previous wing shape and iterating for only 50 more iterations. Fifty iterations required 17 min of execution time on the Control Data CYBER 175 Computer System operating under NOS 1.2.

Results

After extensive iteration on the spanwise variation of profile shape, the sloped pressure distribution was finally achieved across the entire span of the wing. Figure 8 compares the final results for the SMF-2 wing with the results of SMF-1 from figure 3. The expanding flow ahead of the shock wave and a strong shock wave on SMF-1 have been replaced by an isentropic compression and a much weaker shock wave.

The SMF-2 wing achieves the design lift coefficient at the design Mach number by developing a large region of supercritical flow on the wing while still maintaining a reduced shock strength. The Mach number at the crest location (fig. 8) ranges from 1.56 to 1.7 between semispan stations of $\eta = 0.3$ to 0.9. Hence, drag rise due to shock-induced flow separation would not necessarily have to occur with movement of the shock wave aft of the crest when a wing is properly designed.

Selected profile shapes of the two wings are compared in figure 9. By comparing figures 8 and 9, it can be seen that the isentropic compression on SMF-2 is the result of the decreased upper surface streamwise curvature in the midchord region of the wing. The upper surface in this region has been flattened and the curvature has actually been reversed in some areas.

The profile shapes on SMF-2 were defined at eight span stations: $\eta = 0$, 0.2, 0.3, 0.5, 0.8, 0.9, 0.95, and 1.0. It was necessary to define the wing profiles at these span stations to develop the desired pressure distribution. Symmetry of the flow at the root causes the isobars to bend aft and cross perpendicular to the center line. The adjustments to the upper surface curvature in the root region were such as to bring the lift back forward. Outboard of the wing root, the upper surface curvature (and camber) increases in the aft region of the wing and becomes largest at the wing tip. The profile shapes between the root and tip regions are similar to the classical supercritical airfoils of Whitcomb (refs. 18 and 23).

The streamwise thickness distribution was the same at all span stations for SMF-1 and was held fixed during the design of SMF-2. The leading-edge radius of SMF-2 divided by the local chord length is $1.75\ (t/c)^2$ where t/c is the maximum thickness ratio. The thickness included a two-dimensional boundary-layer displacement thickness. Since the pressure distribution is known, the three-dimensional boundary-layer displacement surface could be computed and subtracted from the SMF-2 coordinates in order to determine the actual or "metal" coordinates.

The spanwise variation of twist for SMF-2 is shown in figure 2. According to linear theory, this twist would produce a constant section lift coefficient c_l across most of the span. If the c_l were constant across the span and the same streamwise pressure distribution occurred at all span stations, the isobars would be straightened along lines of constant percent chord. Figure 10 shows the isobar patterns for the two wings at the maneuver condition. Although the twist calculated by linear theory did not produce a constant c_l across the span at these transonic conditions (fig. 11), the streamwise and spanwise load distributions of SMF-2 have resulted in a much straighter isobar pattern. This straightened isobar pattern provides a fuller benefit of sweep over the wing and should reduce the tendency of the flow to separate.

The spanwise distribution of load can be adjusted to achieve a compromise between the induced drag and the drag due to flow separation. Figure 11(a) compares the spanwise load distribution of SMF-2 with an elliptic load at the maneuver condition. A far-field calculation of the induced drag (refs. 32 and 33) shows a penalty of only 3.7 percent above that for an elliptic load.[3] Figure 11(b) shows the spanwise distribution of c_l compared with that required for an elliptic load at the maneuver C_L. The higher c_l near the tip required by the elliptic load would be more likely to produce flow separation in this region due to the presence of a strong shock wave and a large adverse pressure gradient. Thus the reduced likelihood of flow separation with the SMF-2 loading is felt to be worth the penalty in induced drag.

As discussed earlier, the wing shape was tailored to produce a pressure distribution which would reduce shock strength at the high maneuver lift and transonic Mach number. Since the transonic method of Jameson and Caughey does not include such effects as shock—boundary-layer interactions, separation effects, and skin friction, the drag calculations of their computer program are, of course, of limited value. However, it is of some interest to examine the spanwise variation of the calculated drag as an aid in interpreting the near-field drag solution.

Figures 12 and 13 show the effect of Mach number on the spanwise distribution of section drag coefficient at the design C_L for SMF-1 and SMF-2. The

---

[3]Far downstream, the streamwise flow disturbances go to zero so that the nonlinear term disappears from the transonic small disturbance equation. Hence, the linear theory of reference 32 was used to calculate the induced drag in the Trefftz plane by using the load in figure 11(a) corrected to zero at the tip. The program of reference 33 was used.

increment in drag coefficient between the Mach number of 0.90 and 0.01 is plotted for each wing. Although differences in the loading have undoubtedly caused the Δc_d to include some changes in induced drag, the Δc_d distribution generally correlates with the spanwise variation of shock strength for each wing. (See fig. 8.) These results indicate that the wave drag is largest on the outboard part of the wing where the entropy change is the largest, and that Δc_d is some measure of the wave drag. Note that in the outboard region, the Δc_d of SMF-2 is seen to be considerably smaller than for SMF-1.

In order to gain more insight into the general spanwise variation of the drag components, the incompressible drag distribution of SMF-2 has been separated into its components in figure 14. It is recognized, of course, that other components would be present at the design Mach number. Since the three-dimensional transonic theory does not separate the various drag components, the vortex-lattice lifting-surface theory has been utilized to calculate the induced-drag distribution across the wing (near-field solution using the method of ref. 34).[4] A near-field lifting-surface solution has been used since, as pointed out by Garner (ref. 35 or 36), the effect of the chordwise loading on the spanwise distribution of induced drag cannot be calculated by a Trefftz plane or lifting line solution. The effect of the chordwise loading is to cause a high level of induced drag on the inboard part of the wing and thrust on the outboard part, as seen in figure 14. When the induced drag is added to the thickness drag,[5] the result agrees well with the total inviscid drag distribution calculated by the three-dimensional transonic theory.

No attempt has been made to separate the induced drag and the wave drag at the design Mach number. However, the combined results of figures 13 and 14 suggest that the high drag levels occurring over the inboard portion of the wing at $M_\infty = 0.90$ are associated primarily with the effect of the chordwise loading on the induced drag and are not significantly influenced by the wave drag.

CONCLUDING REMARKS

A procedure has been developed which utilizes three-dimensional transonic analysis methods in an iterative fashion for the design of transonic wings. The procedure involves selection of a target pressure distribution and utilizes the principles of both supersonic flow and shock formation and decay to design the wing profile shapes which will approximate the selected pressure distribution.

The method has been illustrated by the design of the wing for a supercritical maneuvering fighter operating at a lift coefficient of 0.86 and a free-stream Mach number of 0.90. In order to achieve high lift and a reduced

---

[4]This distribution of "induced drag" c_d contains the drag due to both the bound vortex system and the trailing vortex system, where the former effect theoretically integrates to zero across the span.

[5]The transonic program was run for zero twist, zero camber, and zero angle of attack and the section drag was interpreted as thickness drag.

shock strength, the wing was designed so that the upper surface flow expands rapidly at the leading edge and isentropically compresses between the leading edge and the shock location.

The requirement for a three-dimensional method in the design of this wing is evidenced by the need to define the wing at eight spanwise stations. Likewise, the detailed analysis of the embedded supersonic flow and shock strength required the use of a nonlinear transonic theory.

A study of the spanwise variation of the inviscid drag components at low speed, coupled with a study of the effect of Mach number on the spanwise distribution of total inviscid drag, suggests that the high drag levels occurring on the inboard portion of the wing at the design Mach number are associated primarily with the effect of chordwise loading on the spanwise distribution of induced drag.

Langley Research Center
National Aeronautics and Space Administration
Hampton, VA 23665
December 15, 1978

REFERENCES

1. Rogers, E. W. E.; and Hall, I. M.: An Introduction to the Flow About Plane Swept-Back Wings at Transonic Speeds. J. Roy. Aeronaut. Soc., vol. 64, no. 596, Aug. 1960, pp. 449-464.

2. Lock, R. C.; and Rogers, E. W. E.: Aerodynamic Design of Swept Wings and Bodies for Transonic Speeds. Vol. 3 of Advances in Aeronautical Sciences, Pergamon Press, Inc., 1961, pp. 253-275.

3. Lock, R. C.: An Equivalence Law Relating Three- and Two-Dimensional Pressure Distributions. R & M. No. 3346, British A.R.C., 1964.

4. Lock, R. C.; and Bridgewater, J.: Theory of Aerodynamic Design for Swept-Winged Aircraft at Transonic and Supersonic Speeds. Vol. 8 of Progress in Aeronautical Sciences, D., Kuchemann, ed., Pergamon Press, Inc., 1966, pp. 139-228.

5. Lock, R. C.: Some Experiments on the Design of Swept Wing Body Combinations at Transonic Speeds. Symposium Transsonicum, Klaus Oswatitsch, ed., Springer-Verlag, 1964, pp. 276-287.

6. Lock, R. C.: The Aerodynamic Design of Swept Winged Aircraft at Transonic and Supersonic Speeds. J. Roy. Aeronaut. Soc., vol. 67, no. 630, June 1963, pp. 325-337.

7. Tulinius, Jan R.; and Margason, Richard J.: Aircraft Aerodynamic Design and Evaluation Methods. AIAA Paper No. 76-15, Jan. 1976.

8. Gingrich, P. B.; Child, R. D.; and Panageas, G. N.: Aerodynamic Configuration Development of the Highly Maneuverable Aircraft Technology Remotely Piloted Research Vehicle. NASA CR-143841, 1977.

9. Gustavsson, Anders L.; and Hedman, Sven G.: Design and Test of a Sonic Roof-Top Pressure Distribution Wing. Symposium Transsonicum II, K. Oswatitsch and D. Rues, eds., Springer-Verlag, 1976, pp. 273-280.

10. Gustavsson, A.; and Vanino, R.: Design and Wind Tunnel Measurement of a Wing-Body Combination With Supercritical Airfoil. NASA TT F-16,916, 1976.

11. Vanino, R.; and Rohlfs, S.: Supercritical Wing Design for a Fighter Type Experimental Aircraft. Symposium Transsonicum II, K. Oswatitsch and D. Rues., eds., Springer-Verlag, 1976, pp. 281-288.

12. Lotz, Michael; and Monnerie, Bernard: The Franco-German Experimental Program for the Evaluation of a Supercritical Wing for a Combat Aircraft Application. ICAS Paper No. 76-21, Oct. 1976.

13. Edwards, David Eugene: A Computational Method for the Design of Transonic Airfoils Using Numerical Optimization. M.S. Thesis, George Washington Univ., 1977.

14. Hicks, Raymond M.; and Vanderplaats, Garret N.: Application of Numerical Optimization to the Design of Supercritical Airfoils Without Drag-Creep. [Preprint] 770440, Soc. Automot. Eng., Mar.-Apr. 1977.

15. Eggleston, B.; and Jones, D. J.: The Design of Lifting Supercritical Airfoils Using a Numerical Optimization Method. Canadian Aeronaut. & Space J., vol. 23, no. 3, May/June 1977, pp. 172-181.

16. Hicks, Raymond M.; and Henne, Preston A.: Wing Design by Numerical Optimization. AIAA Paper 77-1247, Aug. 1977.

17. Ashley, Holt; and Landahl, Marten: Aerodynamics of Wings and Bodies. Addison-Wesley Pub. Co., Inc., c.1965.

18. Whitcomb, Richard T.: Review of NASA Supercritical Airfoils. ICAS Paper No. 74-10, Aug. 1974.

19. Cole, Julian D.: Modern Developments in Transonic Flow. SIAM J. Appl. Math., vol. 29, no. 4, Dec. 1975, pp. 763-787.

20. Murman, E. M.; and Cole, J. D.: Studies in Transonic Flow III. Inviscid Drag at Transonic Speeds. UCLA-ENG-7603, Dec. 1975. (Available as NASA CR-152225.)

21. Mason, William H.; Mackenzie, Donald; Stern, Mark; Ballhaus, William F.; and Frick, Juanita: An Automated Procedure for Computing the Three-Dimensional Transonic Flow Over Wing-Body Combinations, Including Viscous Effects. Volume I - Description of Analysis Methods and Applications. AFFDL-TR-77-122, Vol. I, Feb. 1978. (Available from DDC as AD A055 899.)

22. Von Kármán, Th.: On the Foundation of High Speed Aerodynamics. General Theory of High Speed Aerodynamics. Vol. VI of Series on High Speed Aerodynamics and Jet Propulsion, sec. A. W. R. Sears, ed., Princeton Univ. Press, 1954, pp. 11-12, 23-24.

23. Whitcomb, Richard T.: Advanced Transonic Aerodynamic Technology. Advances in Engineering Science, Volume 4, NASA CP-2001, 1976, pp. 1521-1537.

24. Jameson, Antony: Transonic Flow Calculations. Numerical Methods in Fluid Dynamics, H. J. Wirz and J. J. Smolderen, eds., Hemisphere Pub. Corp., 1978, pp. 1-87.

25. Jameson, Antony; and Caughey, D. A.: Numerical Calculation of the Transonic Flow Past a Swept Wing. COO-3077-140 (Contract EY-76-C-02-3077*000 and NASA Grants NGR-33-016-167 and NGR-33-016-201), Courant Inst. Math. Sci., New York Univ., June 1977. (Available as NASA CR-153297.)

26. Hadley, S. K.; Lydick, L. N.; and Mann, H. W.: Variable Contour, Supercritical, Thin, Fighter Wing Design for Transonic Maneuverability. Rep. No. ERR-FW-1740, General Dynamics, Dec. 31, 1976.

27. Mann, Michael J.: Calculation of the Twist Distribution of Wings Designed for Cruise at Transonic Speeds. NASA TN D-7813, 1974.

28. Dollyhigh, Samuel M.; Ayers, Theodore G.; Morris, Odell A.; and Miller, David M.: Designing for Supercruise and Maneuver. Design Conference Proceedings - Technology for Supersonic Cruise Military Aircraft, Volume I, AFFDL-TR-77-85, Vol. I, U.S. Air Force, 1976.

29. Pearcey, H. H.: The Aerodynamic Design of Section Shapes for Swept Wings. Vol. 3 of Advances in Aeronautical Sciences, Pergamon Press, Inc., 1961, pp. 277-322.

30. Pearcey, H. H.: Some Aspects of the Physical Nature of Transonic Flows Past Aerofoils and Wings. Symposium Transsonicum, Klaus Oswatitsch, ed., Springer-Verlag, 1964, pp. 264-275.

31. Liepmann, H. W.; and Roshko, A.: Elements of Gasdynamics. John Wiley & Sons, Inc., c.1957.

32. Multhopp, H.: Methods for Calculating the Lift Distribution of Wings (Subsonic Lifting-Surface Theory). R. & M. No. 2884, British A.R.C., Jan. 1950.

33. Lamar, John E.: A Modified Multhopp Approach for Predicting Lifting Pressures and Camber Shape for Composite Planforms in Subsonic Flow. Supplement to NASA TN D-4427, 1968.

34. Margason, Richard J.; and Lamar, John E.: Vortex-Lattice FORTRAN Program for Estimating Subsonic Aerodynamic Characteristics of Complex Planforms. NASA TN D-6142, 1971.

35. Garner, H. C.: Some Remarks on Vortex Drag and its Spanwise Distribution in Incompressible Flow. NPL Aero Note 1048, British A.R.C., Nov. 4, 1966.

36. Garner, H. C.: Some Remarks on Vortex Drag and its Spanwise Distribution in Incompressible Flow. Aeronaut. J., vol. 72, no. 691, July 1968. pp. 623-625.

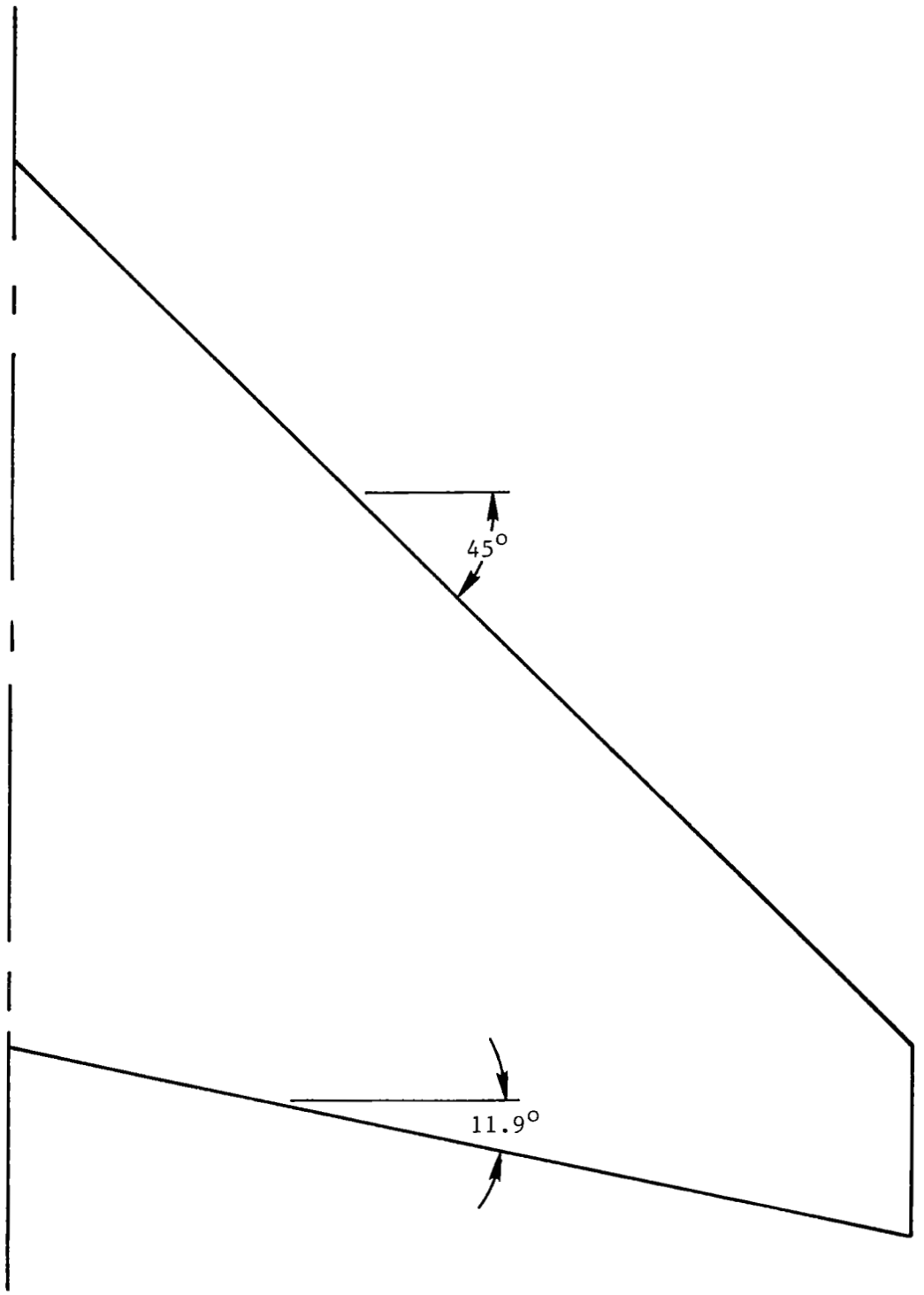

Figure 1.- Planform with aspect ratio, 3.28; taper ratio, 0.2142; and maximum thickness ratio, 0.0465.

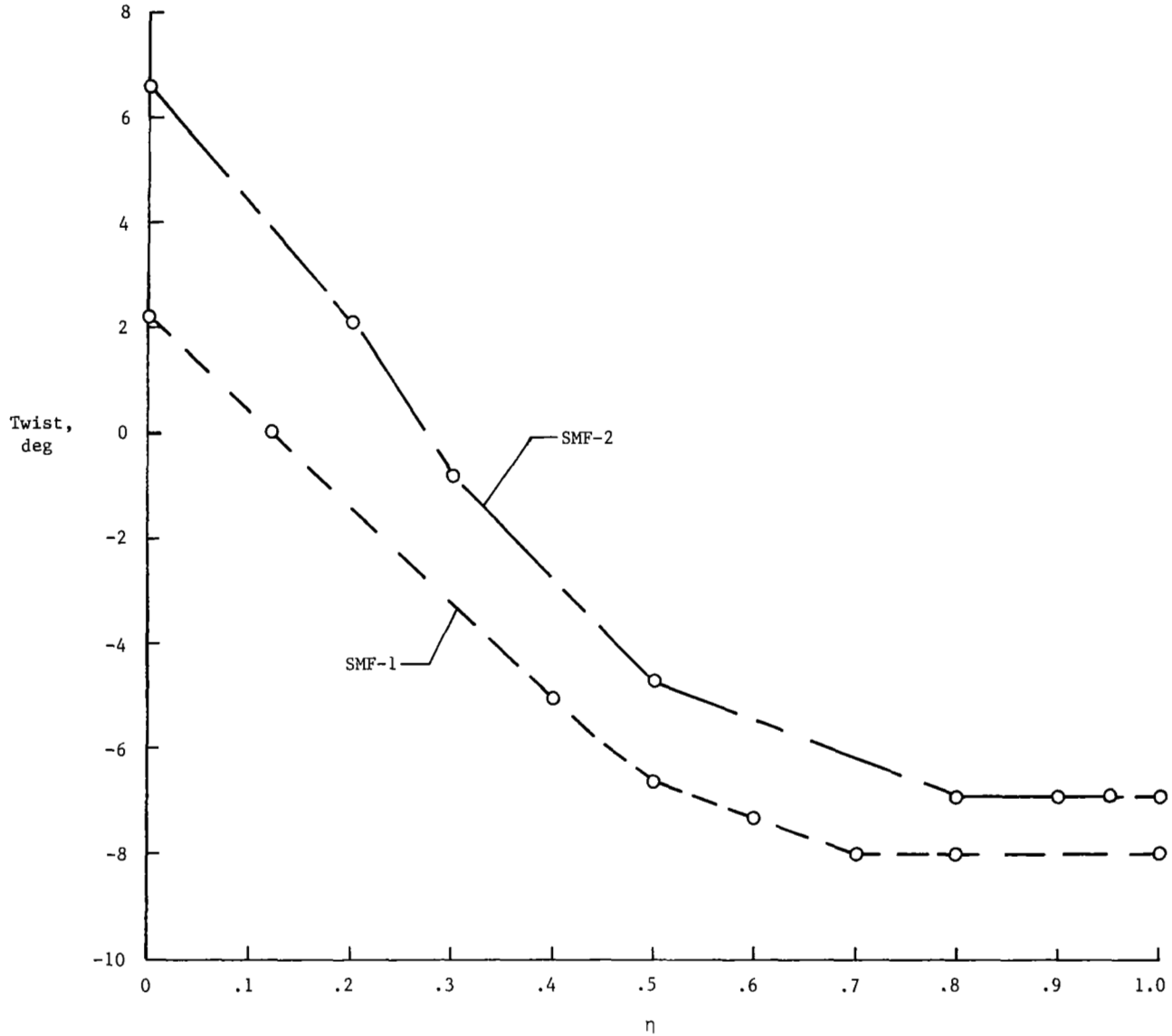

Figure 2.- Twist distributions.

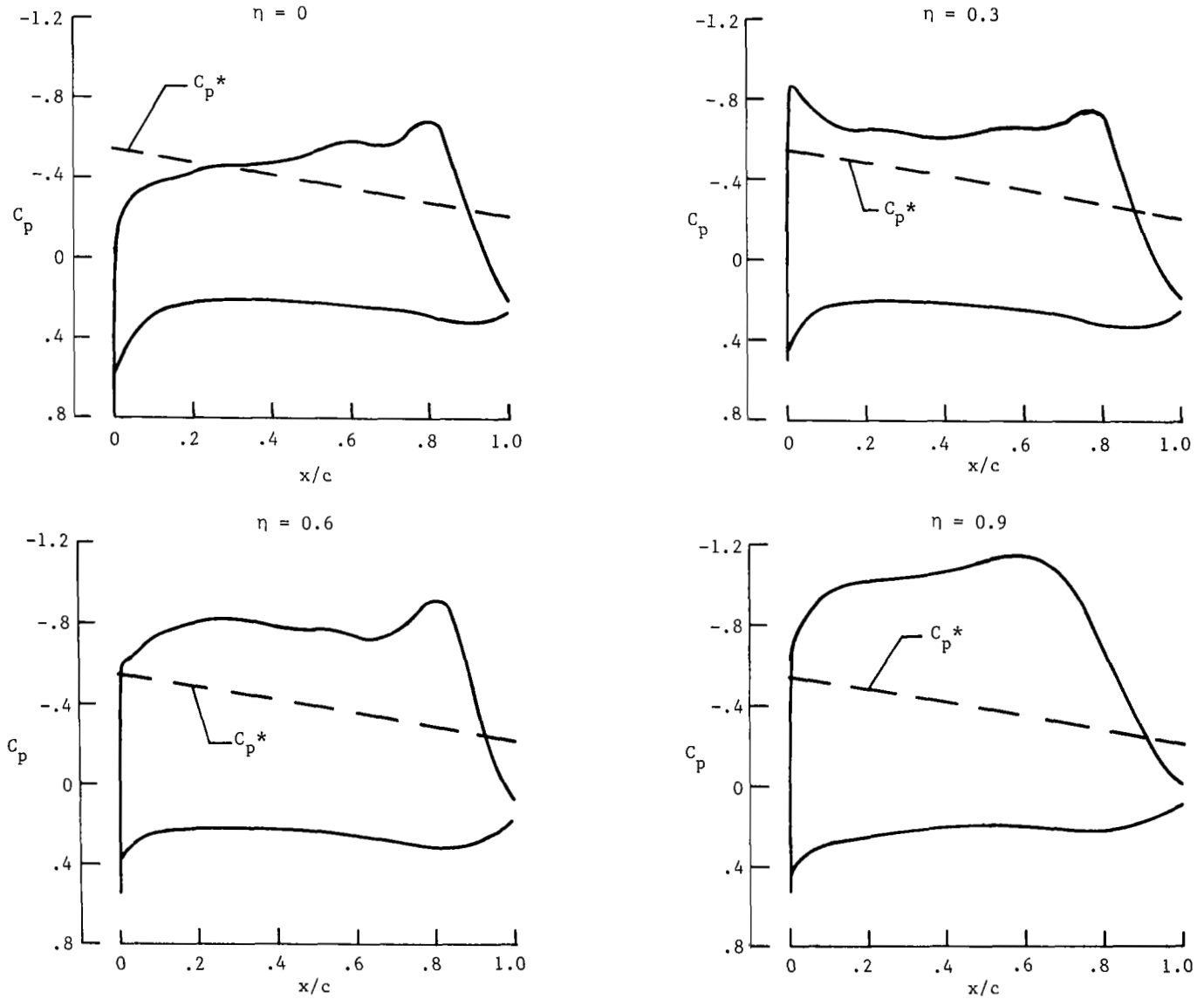

Figure 3.- Pressure distributions for SMF-1 at $M_\infty = 0.90$, $C_L = 0.86$, and $\alpha = 9.6^o$.

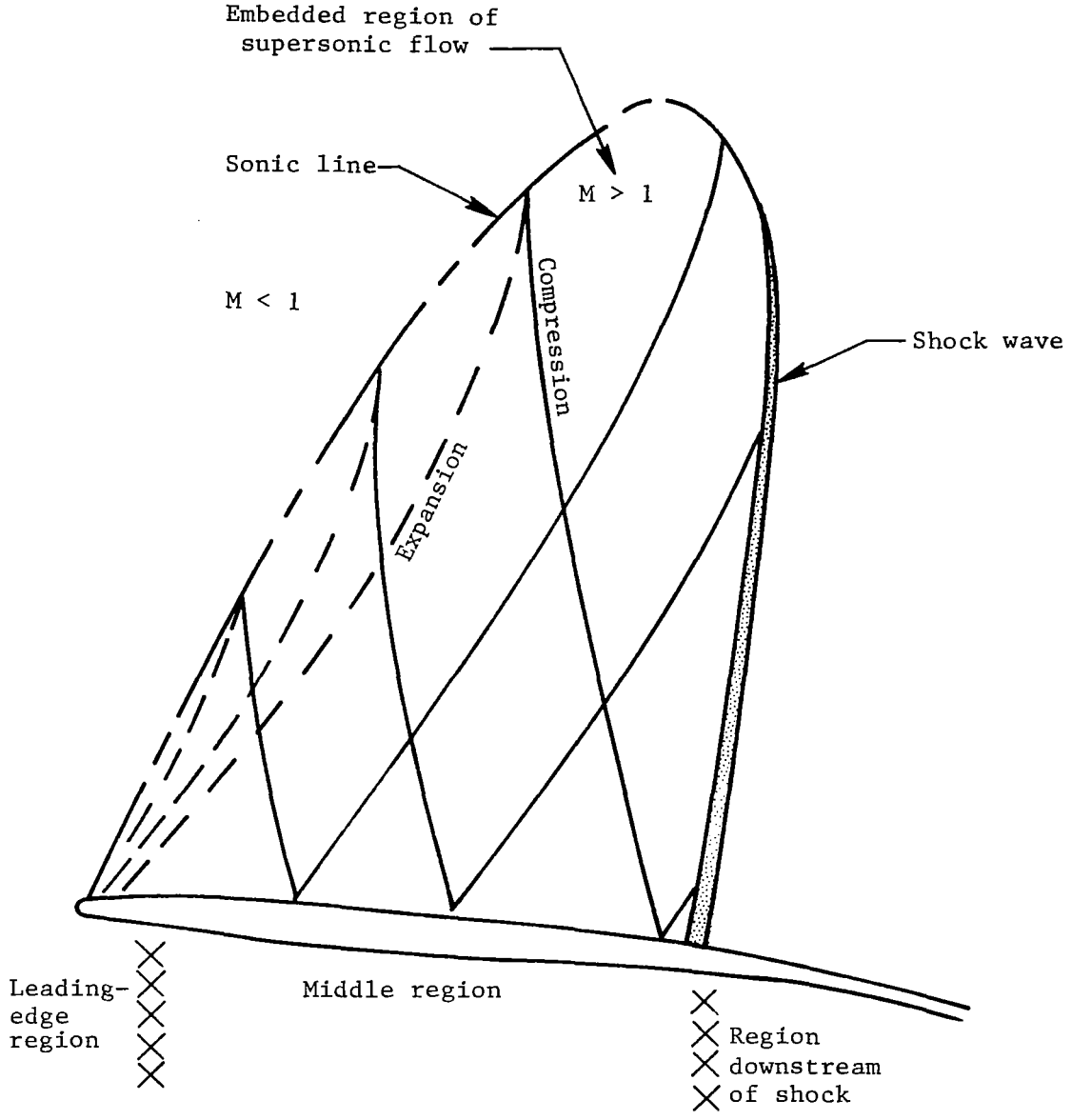

Figure 4.- Three chordwise regions used in design method and effect of an expansion wave coming from the first or leading-edge region. (Waves originating at other locations along the chord are not shown.)

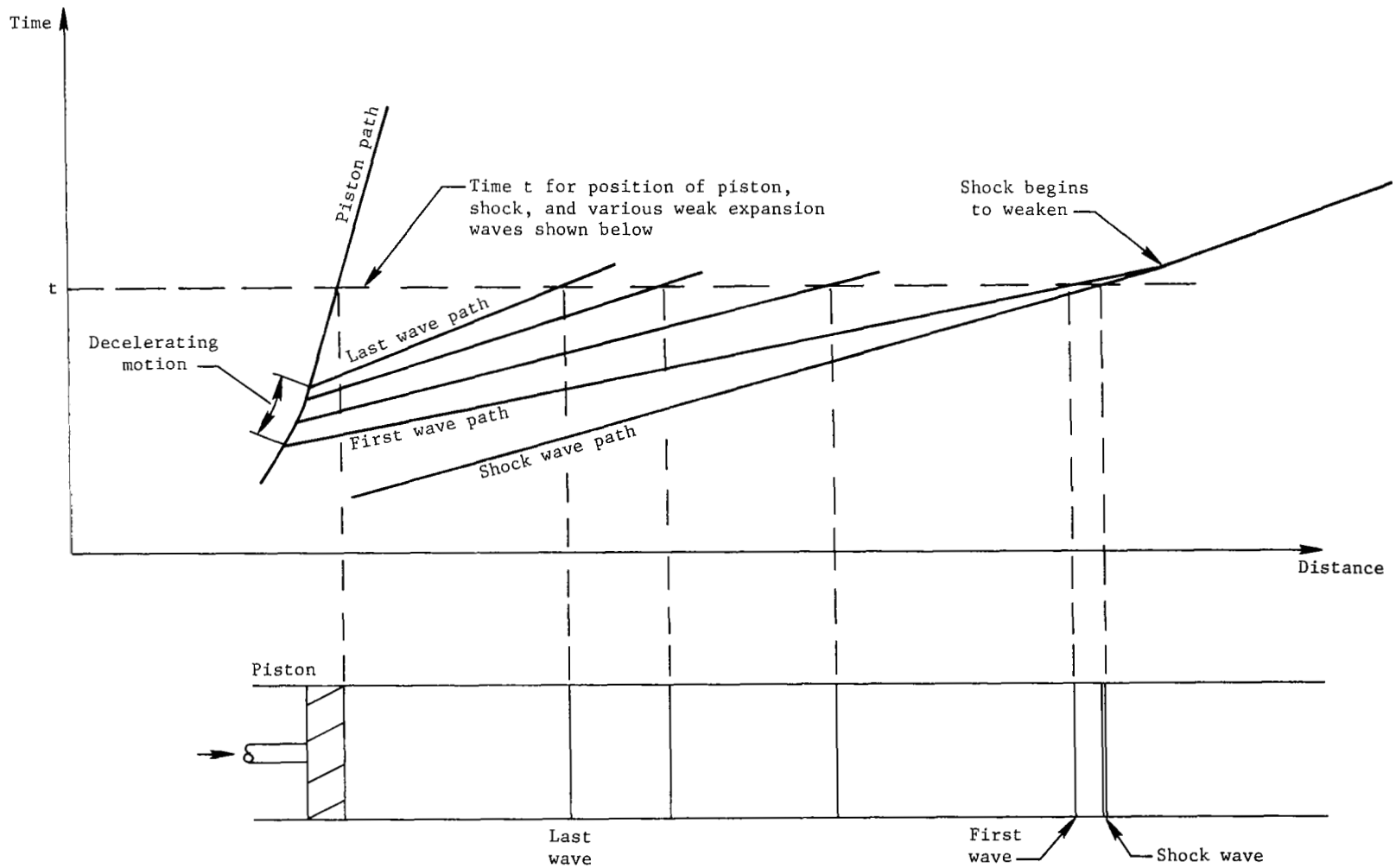

Figure 5.- A decelerating piston forms weak expansion waves which diverge but always catch previously formed shock wave and reduce its strength.

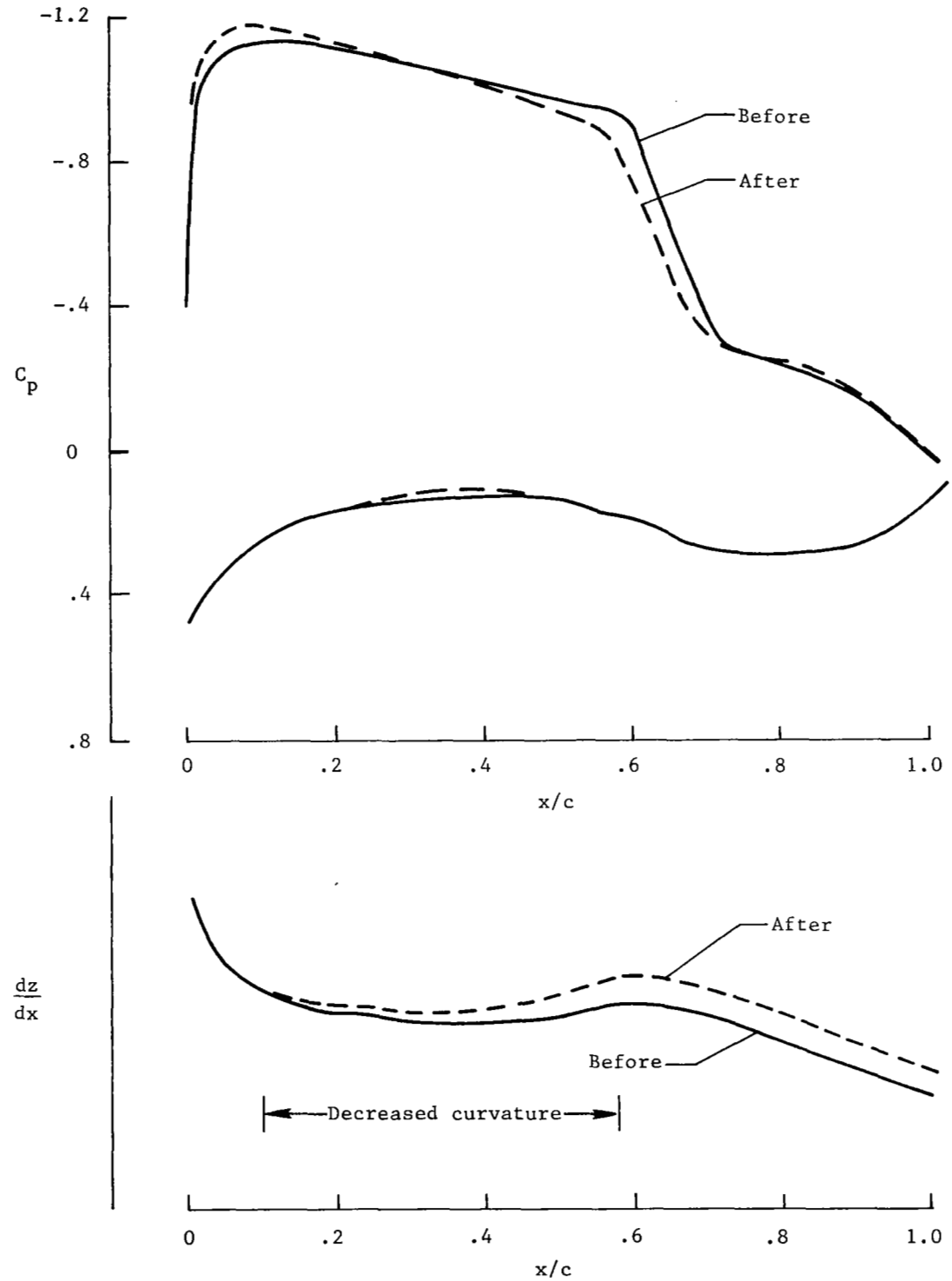

Figure 6.- Decrease in upper surface curvature to increase isentropic compression in middle region and reduce shock strength; $\eta = 0.8$.

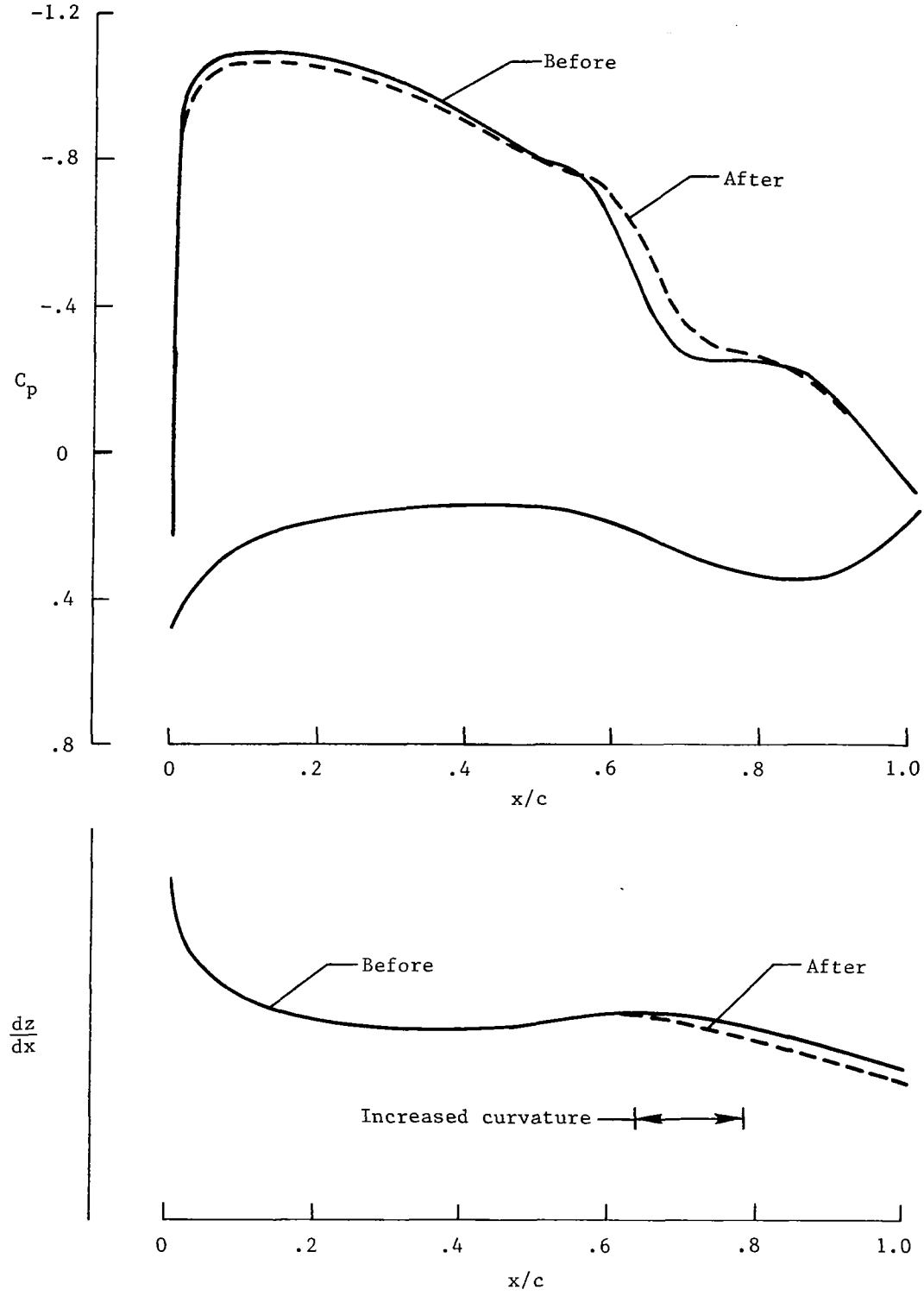

Figure 7.- Increase in curvature at, and just downstream of, shock to reduce shock strength; $\eta = 0.5$.

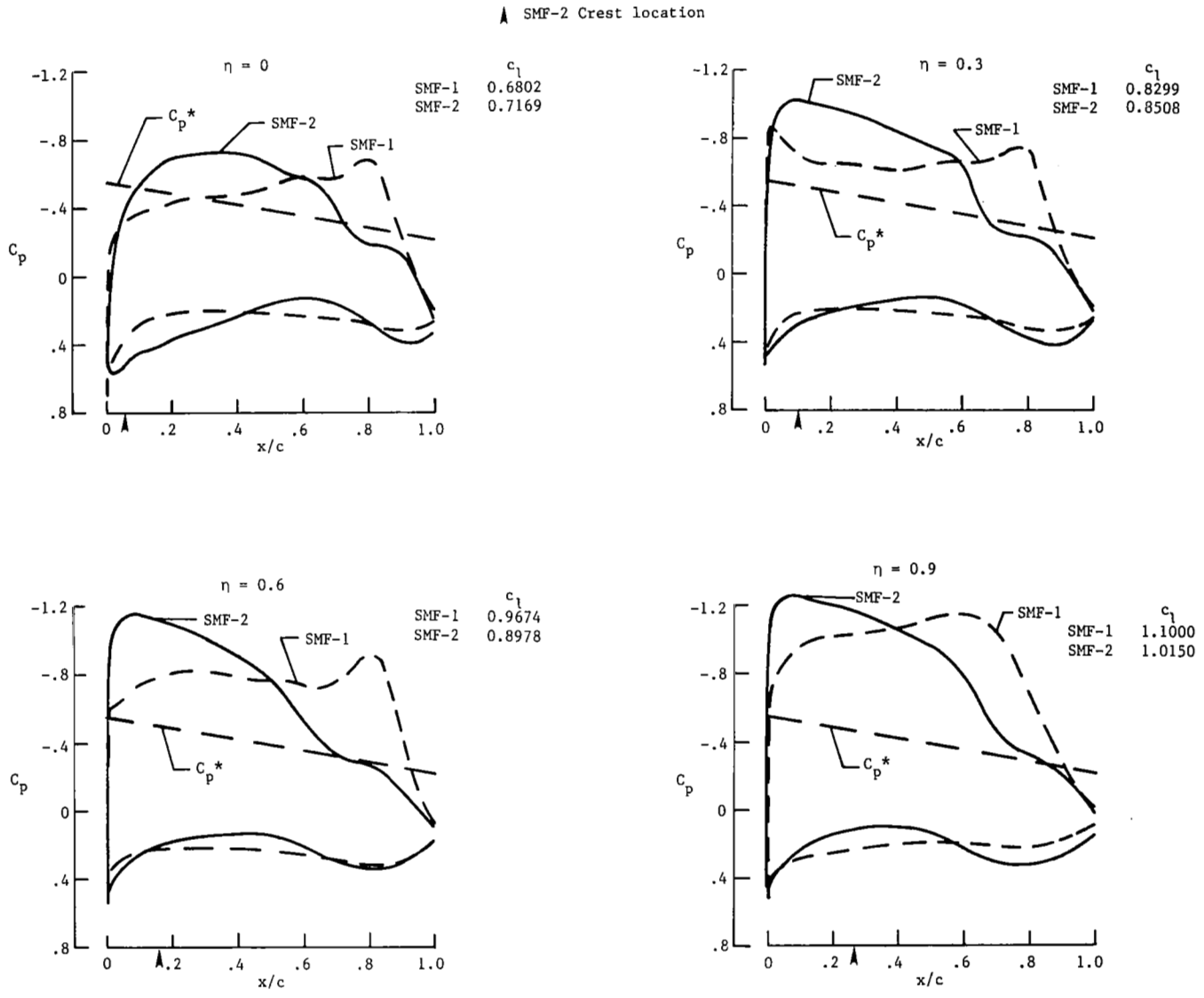

Figure 8.- Pressure distributions for SMF-2 compared with those for SMF-1 at $M_\infty = 0.90$ and $C_L = 0.86$. For SMF-1, $\alpha = 9.6^o$; for SMF-2, $\alpha = 7.45^o$.

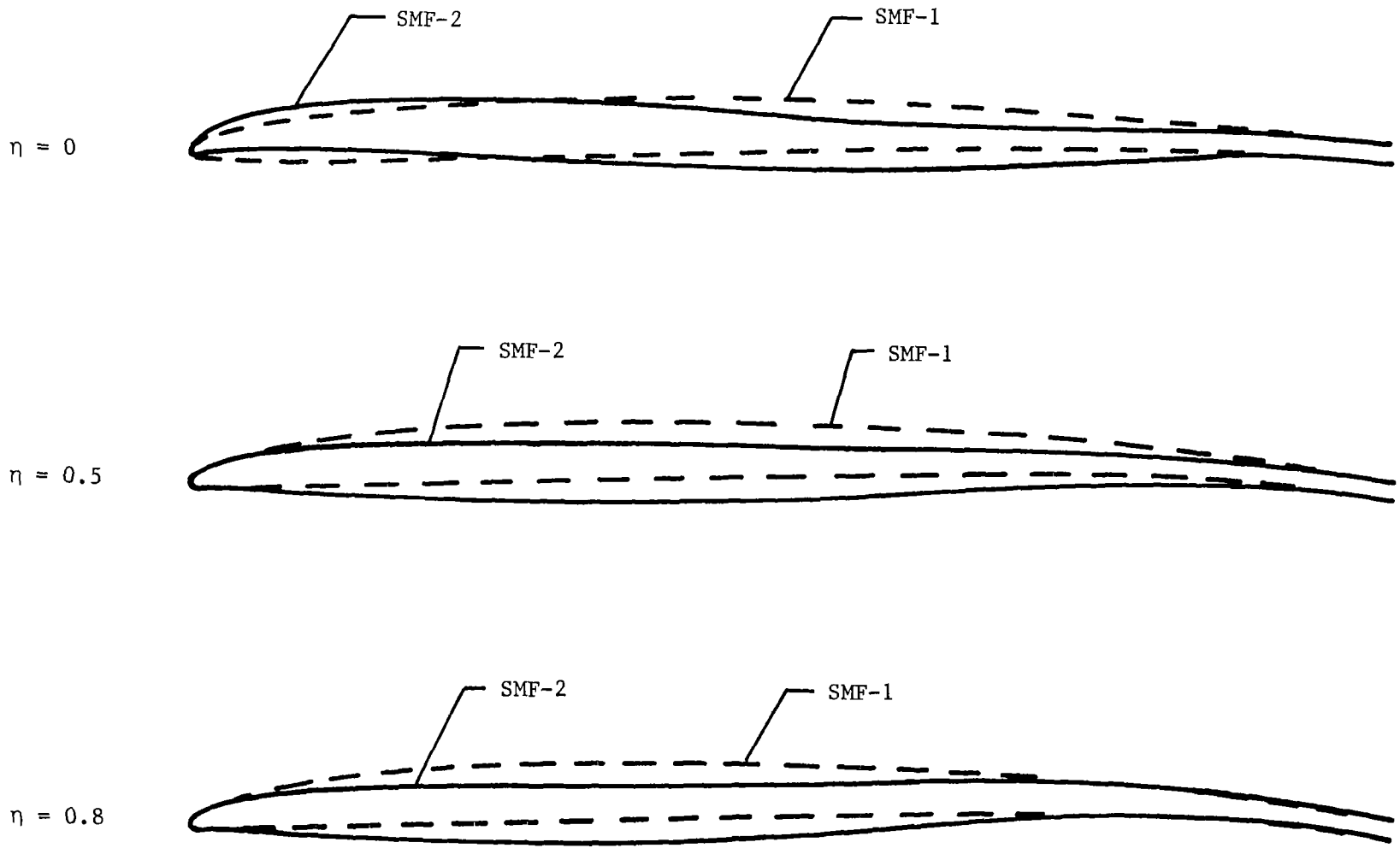

Figure 9.- Profile shapes for SMF-1 and SMF-2.

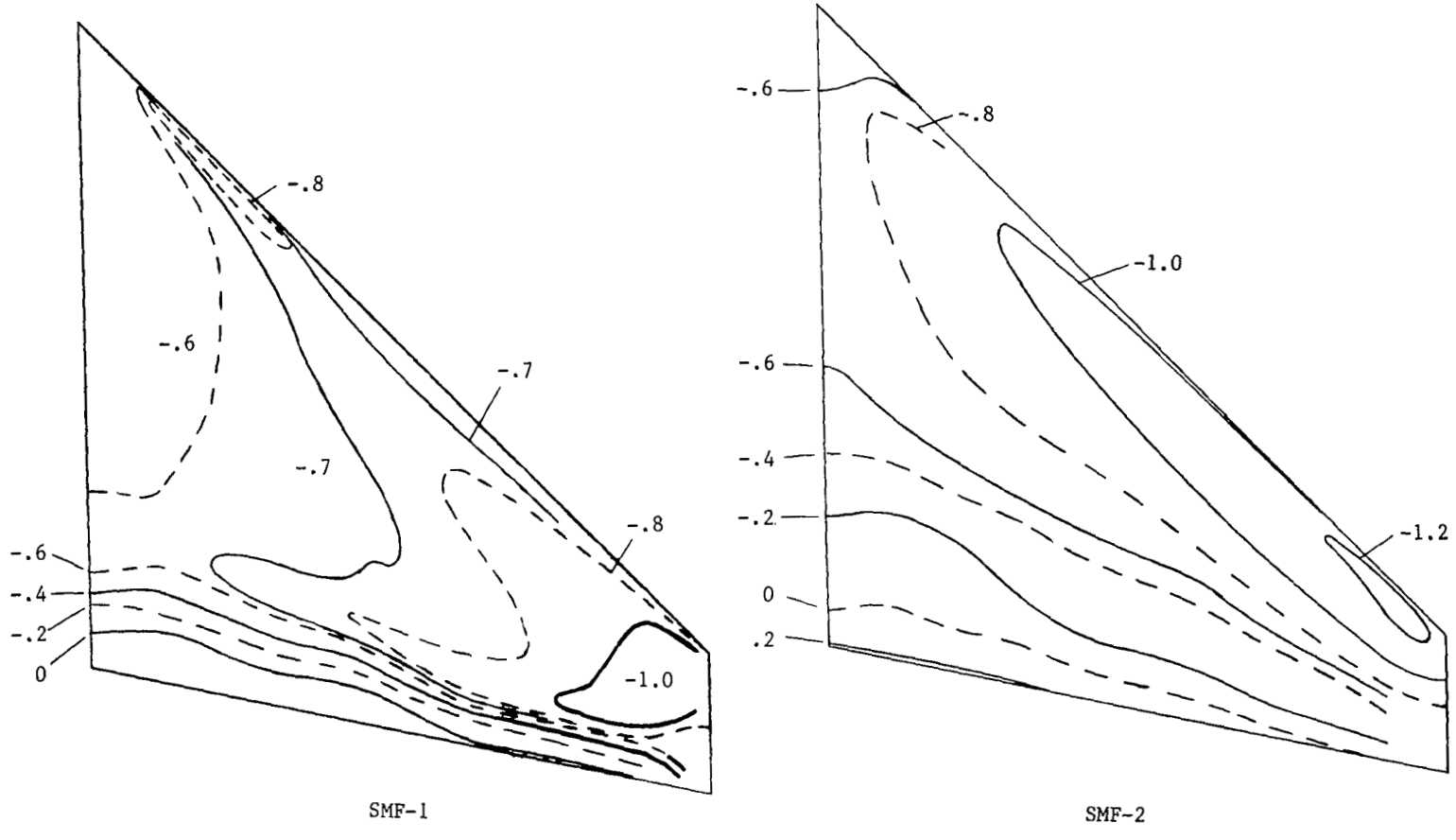

Figure 10.- Upper surface isobar patterns for SMF-1 and SMF-2 for $C_L = 0.86$ and $M_\infty = 0.90$.

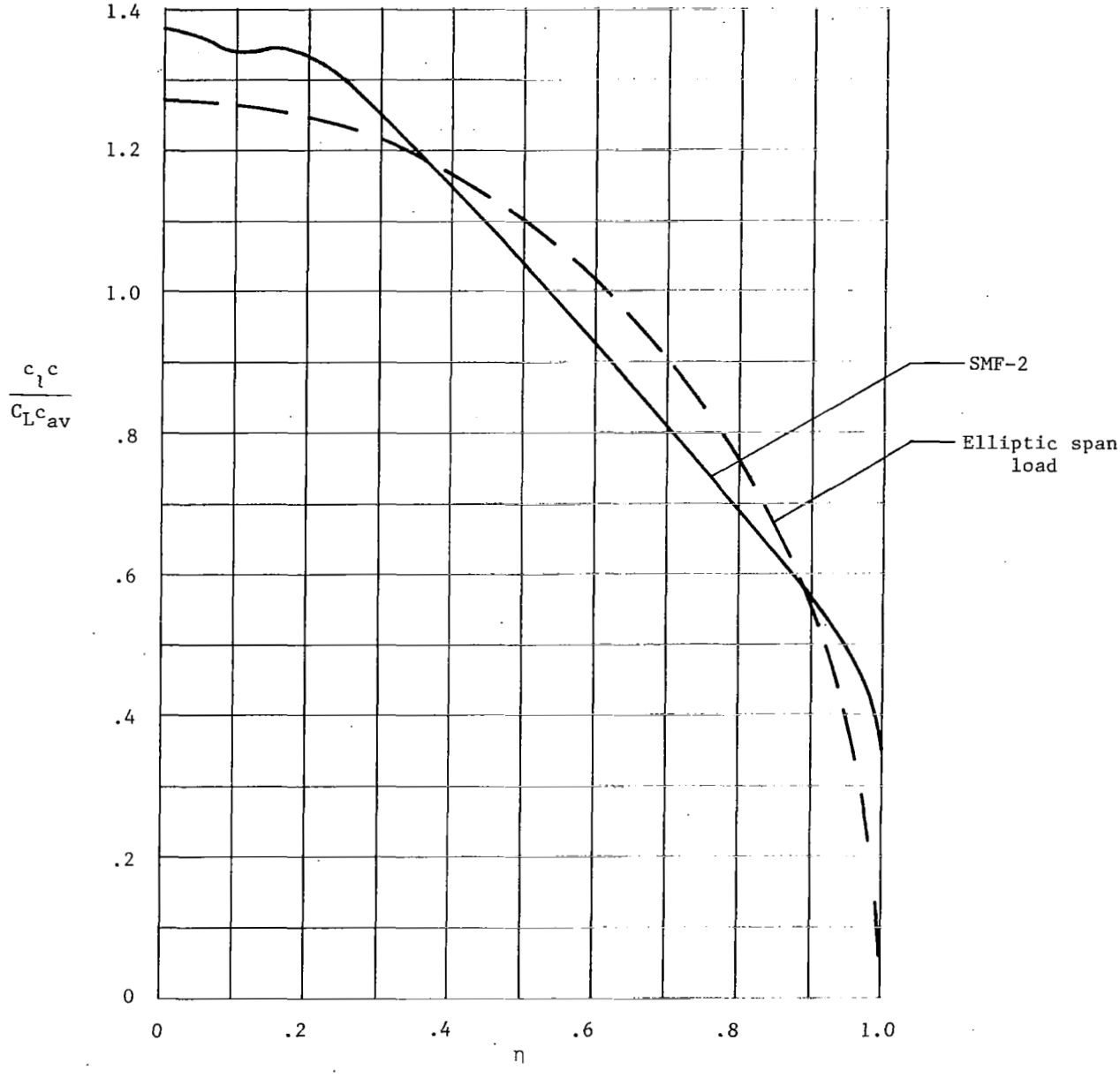

(a) Spanwise load distribution.

Figure 11.- Spanwise distribution of load and lift on SMF-2 at $M_\infty = 0.90$ and $C_L = 0.8576$ compared with case of an elliptic load distribution.

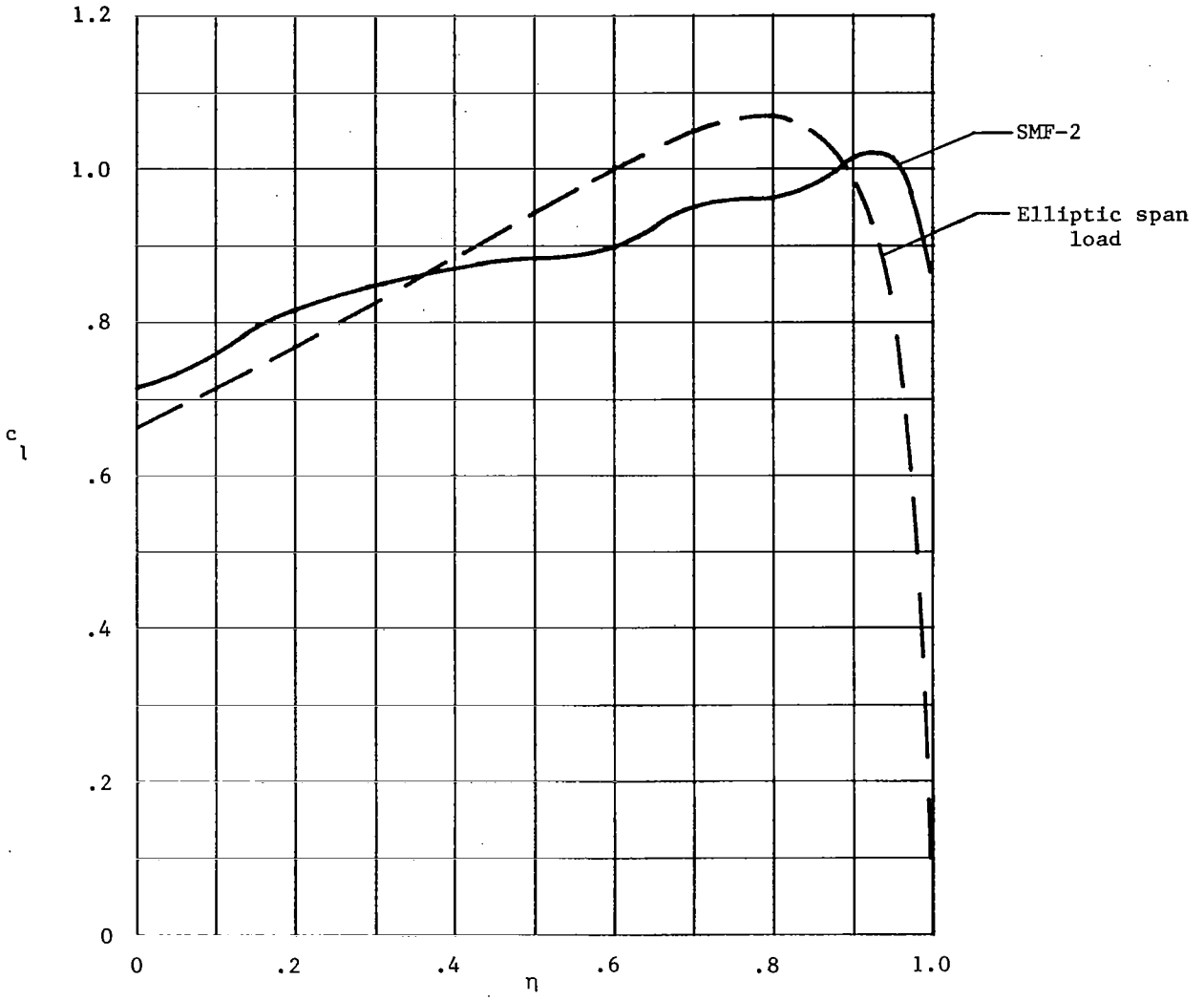

(b) Spanwise lift distribution.

Figure 11.- Concluded.

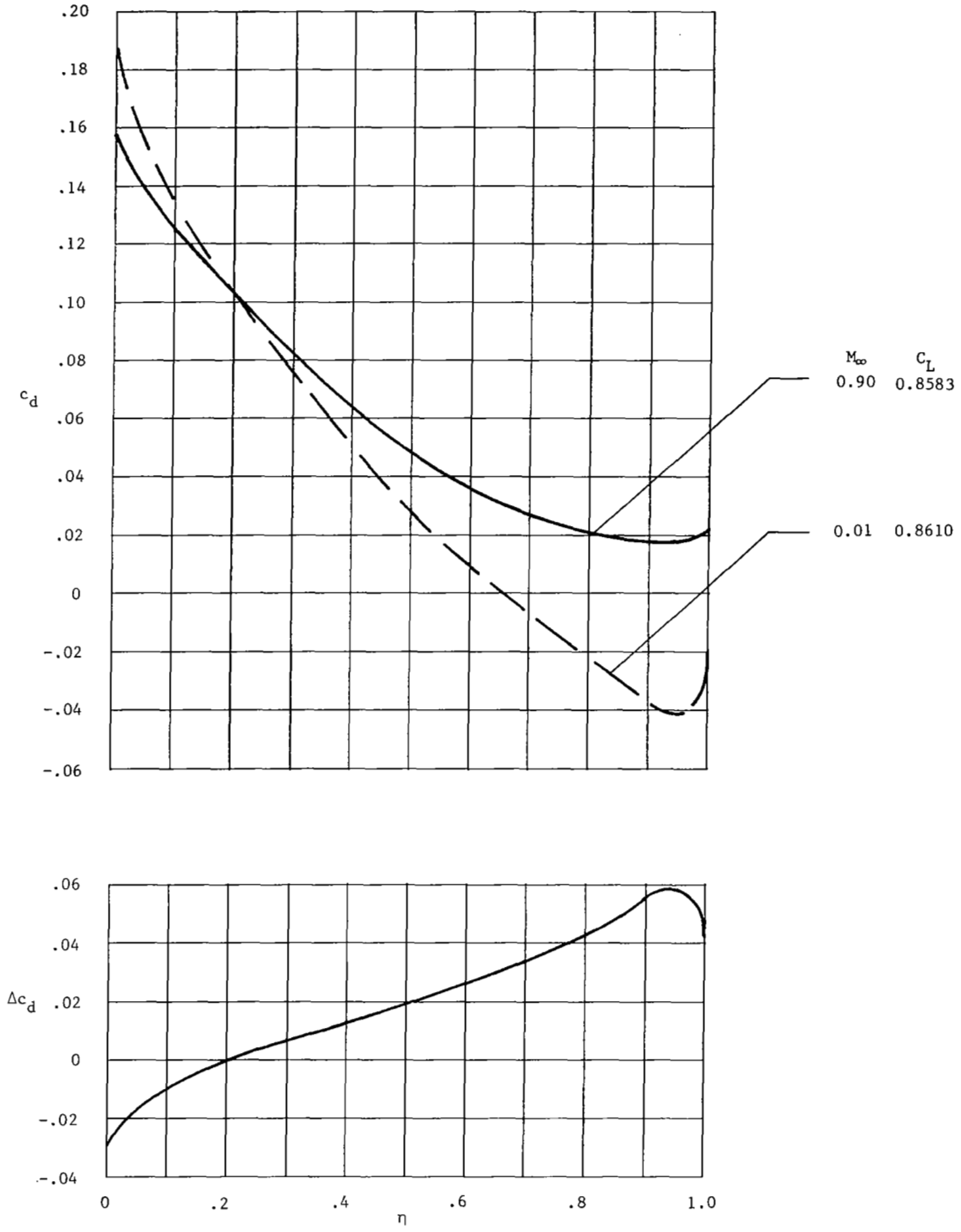

Figure 12.- Effect of Mach number on spanwise distribution of drag for SMF-1 as determined by three-dimensional transonic theory (refs. 24 and 25).

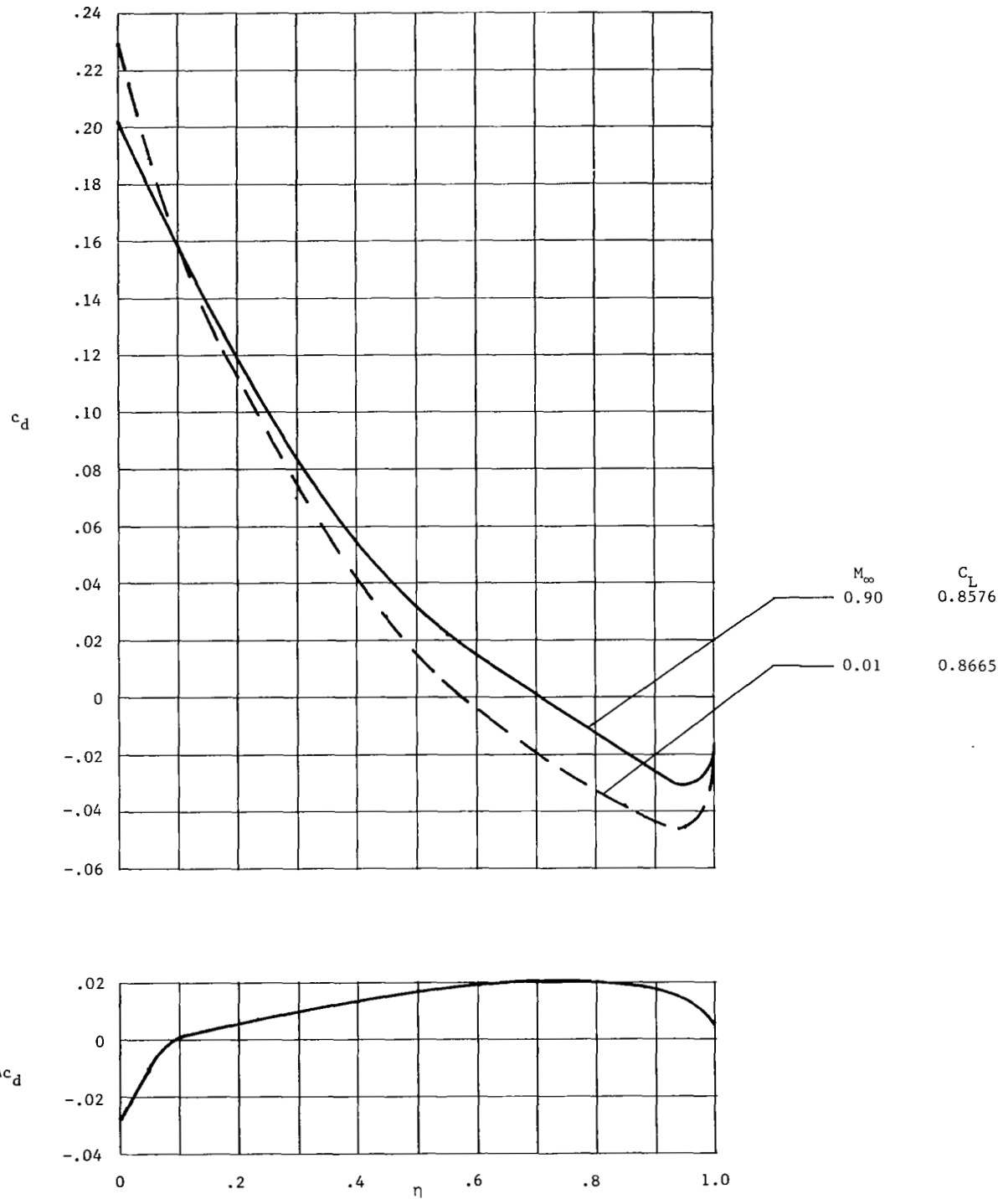

Figure 13.- Effect of Mach number on spanwise distribution of drag for SMF-2 as determined by three-dimensional transonic theory (refs. 24 and 25).

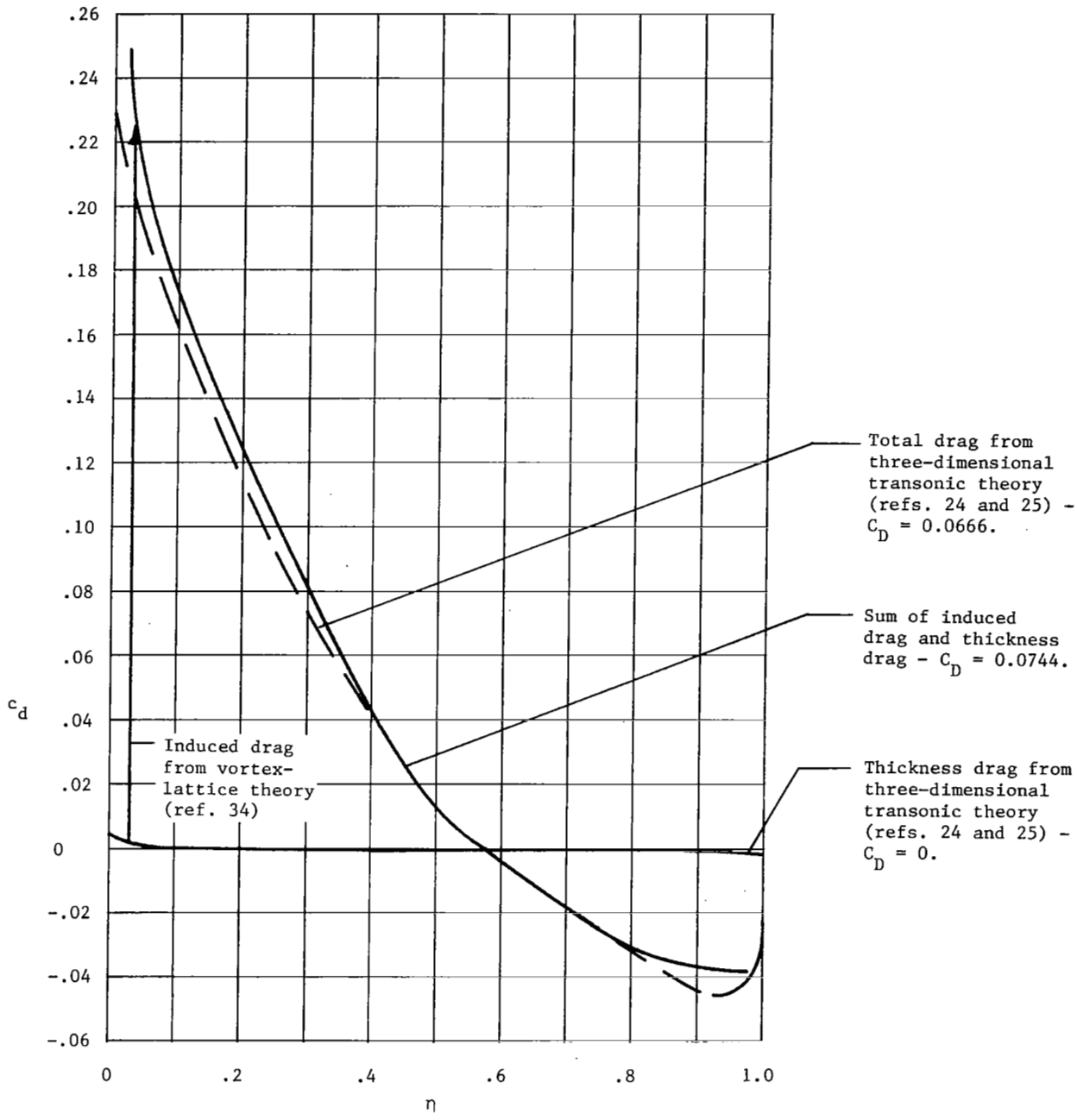

Figure 14.- Spanwise variation of drag components on SMF-2 for $M_\infty = 0.01$ and $C_L = 0.8665$.

1. Report No.	2. Government Accession No.	3. Recipient's Catalog No.
NASA TP-1400		

4. Title and Subtitle	5. Report Date
THE DESIGN OF SUPERCRITICAL WINGS BY THE USE OF THREE-DIMENSIONAL TRANSONIC THEORY	February 1979
	6. Performing Organization Code
7. Author(s)	8. Performing Organization Report No.
Michael J. Mann	L-12552
	10. Work Unit No.
9. Performing Organization Name and Address	505-11-13-03
NASA Langley Research Center Hampton VA 23665	11. Contract or Grant No.
	13. Type of Report and Period Covered
12. Sponsoring Agency Name and Address	Technical Paper
National Aeronautics and Space Administration Washington, DC 20546	14. Sponsoring Agency Code

15. Supplementary Notes

16. Abstract

A procedure has been developed for the design of transonic wings by the iterative use of three-dimensional, inviscid, transonic analysis methods. The procedure is based on simple principles of supersonic flow and provides the designer with a set of guidelines for the systematic alteration of wing profile shapes to achieve some desired pressure distribution. The method is generally applicable to wing design at conditions involving a large region of supercritical flow. To illustrate the method, it is applied to the design of a wing for a supercritical maneuvering fighter that operates at high lift and a transonic Mach number. The wing profiles were altered to produce a large region of supercritical flow which is terminated by a weak shock wave. The spanwise variation of drag of this wing and some principles for selecting the streamwise pressure distribution are also discussed.

17. Key Words (Suggested by Author(s))	18. Distribution Statement
Transonic wing design Wing design Supercritical wing design Maneuvering fighter Supercritical maneuvering fighter Supercritical fighter	Unclassified - Unlimited Subject Category 02

19. Security Classif. (of this report)	20. Security Classif. (of this page)	21. No. of Pages	22. Price*
Unclassified	Unclassified	30	$4.50

* For sale by the National Technical Information Service, Springfield, Virginia 22161

NASA-Langley, 1979